Progress in Measuring Simulation Fidelity using an Adaptive Pilot Model

Mark D White
Manager, Flight Simulation Laboratory
mdw@liv.ac.uk

Gareth D Padfield
Professor of Aerospace Engineering
gareth.padfield@liv.ac.uk

Robert Armstrong
Research Student
r.armstrong@liv.ac.uk

Flight Science and Technology
The University of Liverpool
Liverpool, United Kingdom

Abstract

The paper reports developments in a new approach to the quantification of simulation fidelity based on an analysis of pilot motion control strategy. Manoeuvre guidance is modelled as the solution to a low order equivalent system, wherein the model parameters are allowed to vary to account for pilot adaptation during the manoeuvre, described as the adaptive pilot model (APM). In the paper the theoretical foundation to the concept is developed using the familiar spatial variables in flight control, such as distance and speed, and also temporal variables particularly $\tau(t)$ - the instantaneous time to contact. Using the theory of $\tau(t)$-coupling from visual flow theory, the APM can be transformed into a rather simple algebraic relationship when the pilot maintains constant $\dot{\tau}$ during a deceleration. Alternatively, during a complete acceleration-deceleration manoeuvre, evidence is provided for a different strategy based on the pilot following a constant acceleration τ guide. Assuming a separation of guidance and stabilisation control strategies, pilot guidance feedback gains are then closely related to the frequency and damping of the APM structure. Results are presented from the analysis of data from simulation trials with pilots flying an acceleration-deceleration manoeuvre that show close correlation with the $\tau(t)$-based guidance strategy. However, differences between the interpretation of pilot control strategy predicted by the spatial and temporal models remain unresolved, forming the motivation for continuing research. The relevance of the theory to simulation fidelity criteria is discussed.

Symbols

C	coupling constant
g	gravitational constant
K_R	pilot gain relating pitch attitude command to range error
$K_{\dot{R}}$	pilot gain relating pitch attitude command to range rate
k	τ coupling parameter
R	range
R_c	range command (= X_0)
s	Laplace transform variable
$t, \bar{t}$	time and normalised time (by T)
t_r	time at pitch attitude reversal
T	manoeuvre time
$X, \bar{X}$	distance to go, distance to go normalised by total distance
$\dot{X}, \bar{X}'$	rate of change of distance to go (velocity), velocity normalised by total distance
$\ddot{X}, \bar{X}''$	acceleration, acceleration normalised by total distance
X_g	distance to go for tau-guide
X_u	drag derivative
$Y_{A\theta}$	aircraft transfer function between pitch attitude and range
$Y_{P\theta}$	pilot transfer function between pitch angle and pitch command
Y_{PR}	pilot transfer function between range error and pitch command
$\tau(t)$	time to contact
τ_X	time to stop in manoeuvre
τ_g	time to stop for a tau-guide
$\dot{\tau}$	rate of change of τ with time
$\tau_\theta, \omega_\theta$	time constant and bandwidth in pilot attitude stabilisation model
θ, θ_c	pitch attitude, pitch attitude command
ω_R, ω_X	natural frequency in the adaptive pilot model structure
ζ_R, ζ_X	relative damping in the adaptive pilot model structure

Introduction

The level of fidelity of Synthetic Training Devices (STD) is quantified in JAR-STD-1H (Ref 1) in terms of performance criteria for the individual components, e.g. the motion/visual/sound systems, the mathematical model. Ref 1 also requires piloted assessment of the integrated system with typical mission sorties flown covering the training aspects for which the system will be used. Pilot subjective opinion reflects the value that an experienced pilot places on the level of realism. Quantifying overall simulation fidelity is more difficult, but is equally important. Arguably, component fidelity can only be properly related to fitness for purpose if connected by measure to the integrated synthetic system. This paper reports progress in the development of an approach for quantifying overall simulation fidelity based on an analysis of pilot visual guidance strategy - identifying the control loops utilised, levels of abruptness and the cues available to support anticipation. The premise is that if the control strategy adopted to perform a flying task is 'equivalent' in flight and simulation, then the fidelity is good and the training device fit for purpose. The meaning of equivalent is developed in terms of what can be described as the *Adaptive Pilot Model* (APM), whereby the combined pilot and aircraft is modelled as an equivalent system (Ref 2). Comparisons made of model parameters identified from the same curve fitting process applied to data from flight and simulation tests then form the basis of system fidelity. In the APM approach, the changing pilot gains relating to velocity and distance control, for example, are tracked through the manoeuvre. The concept can be extended under the premise that motion control by the pilot follows temporal rather than spatial guidance principles; the idea being that pilots strictly have no need for velocity or distance information, per se, when manoeuvring close to a surface. Instead, they use information about time to close on surfaces, $\tau(t)$, to make judgements about relative motion and the associated control requirements. The APM structure and temporal guidance approach is illustrated with reference to an acceleration-deceleration manoeuvre. Results are shown for several test cases from flight simulation with the visual cues modified to give different usable cue environments.

The theoretical foundations of the Adaptive Pilot Model concept as applied to the manoeuvres under investigation are developed and results are presented from flight simulation tests with the FLIGHTLAB Bo105 model. The results are discussed in relation to closed loop fidelity criteria. Future directions of the research activity are outlined, followed by concluding remarks.

Theoretical Foundations of the APM

The general hypothesis behind the adaptive pilot model follows from earlier representations (Refs 2-4), whereby, in flying a manoeuvre, the pilot acts to transform the coupled aircraft-pilot system to a simple relationship between command and output. In the acceleration-deceleration manoeuvre, for example, the pilot initiates the manoeuvre from a hover in response to the command R_c and finishes in a new hover when the error $(R_c\text{-}R)$ is reduced to zero (Fig 1). The distance to stop is defined as $-X$.
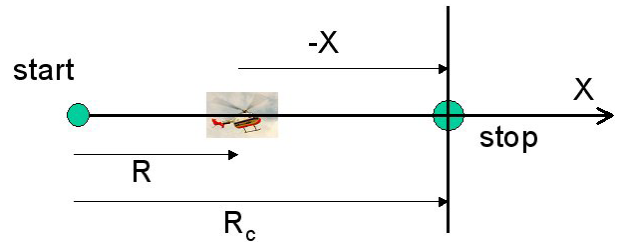

Figure 1 Kinematics of the Accel-Decel Manoeuvre

In Fig 2, portraying the closed loop control scheme, θ_c is the commanded pitch attitude and θ is the current pitch attitude.
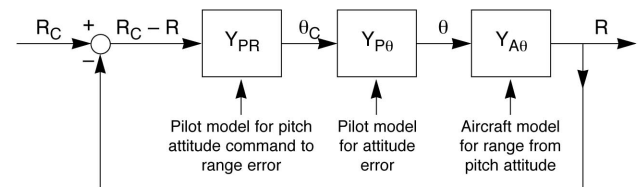

Figure 2 Closed-loop Control of Aircraft Range

A transfer function representation is used for convenience at this stage, recognising that the nonlinear, time-dependent nature of the APM precludes this approach. The pilot guidance transfer function Y_{PR} is assumed to take the form of proportional and rate feedback (K_R and $K_{\dot{R}}$) on range error;

$$Y_{PR} = -K_R - K_{\dot{R}}s \qquad (1)$$

The transfer function $Y_{P\theta}$ represents the pilot-aircraft, short-term pitch dynamics (stabilisation

function) and is assumed to take the form of a first order lag with time constant τ_θ (bandwidth ω_θ).

$$Y_{P\theta} = \frac{1}{1+\tau_\theta s} \qquad (2)$$

The aircraft transfer function between range response and pitch attitude is approximated in first order form, including the drag derivative X_u;

$$Y_{A\theta} = \frac{-g}{s(s-X_u)} \qquad (3)$$

The open loop transfer function between range error and range is then given by;

$$Y = Y_{PR} \, Y_{P\theta} \, Y_{A\theta} =$$
$$= -\frac{g}{s(s-X_u)} \frac{1}{(1+\tau_\theta s)} (K_R + K_{\dot{R}}s) \qquad (4)$$

The dynamics of the free response of the system to a displaced initial range are defined by the solutions to the equation $1+Y=0$, or;

$$\frac{s^3}{\omega_\theta} + \left(1-\frac{X_u}{\omega_\theta}\right)s^2 + \left(gK_{\dot{R}}-X_u\right)s + gK_R = 0 \qquad (5)$$

Applying the further approximation that the closed loop attitude dynamics are much faster than the translational dynamics (i.e. stabilisation much faster than guidance), and that $\omega_\theta >> -X_u$, so that a constant pitch attitude gives a constant acceleration or deceleration, the system reduces to 2nd order form,

$$s^2 + 2\zeta_R \omega_R s + \omega_R^2 = 0 \qquad (6)$$

where the pilot gains are related to the natural frequency ω_R and damping ratio ζ_R by the expressions,

$$K_{\dot{R}} \approx \frac{2\zeta_R \omega_R}{g} \qquad K_R \approx \frac{\omega_R^2}{g} \qquad (7)$$

Expressed as an initial value problem in terms of the distance to go X, the APM takes the form;

$$\frac{d^2 X}{dt^2} + 2\zeta_X \omega_X \frac{dX}{dt} + \omega_X^2 X = 0, \qquad (8)$$
$$X(0) = -R_c$$

The model can also be expressed in terms of the time to go in the manoeuvre, $\tau(t)$,

$$\tau(t) = \frac{X}{\dot{X}} \qquad (9)$$

In the natural world, the time to go information can readily be scaled in terms of eye-heights, and using a combination of surface and object $\tau(t)$'s, afford animals (and pilots) with knowledge of the height of the surrounding terrain with respect to themselves (Refs 5, 6).

The rate of change of $\tau(t)$ with time can be obtained by differentiating eqn (9), giving,

$$\dot{\tau} = 1 - \frac{X\ddot{X}}{\dot{X}^2} \qquad (10)$$

Multiplying eqn (8) by $\frac{X}{\dot{X}^2}$ and combining with eqn (10), the APM can be written in the form,

$$\frac{X\ddot{X}}{\dot{X}^2} = 1 - \dot{\tau} = -2\zeta_X(\omega_X \tau) - (\omega_X \tau)^2 \qquad (11)$$

or

$$\dot{\tau} - 1 = 2\zeta_X(\omega_X \tau) + (\omega_X \tau)^2 \qquad (12)$$

The quadratic relationship in eqn (12) holds for the whole manoeuvre, with the general solution given by,

$$\omega_X \tau = -\zeta_X \pm \sqrt{\zeta_X^2 + (\dot{\tau}-1)} \qquad (13)$$

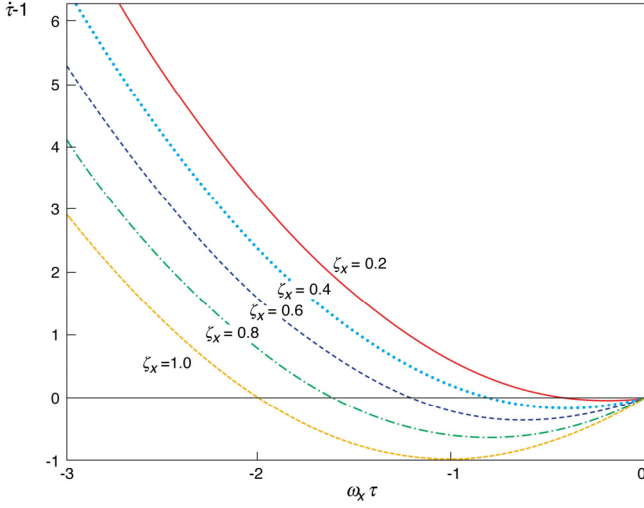The solution to equation (12) is shown in Fig 3, for various values of damping ratio ζ_X.

Figure 3 Motion Profiles in the τ-domain

Some important features of the variations shown include;

  a) If the damping ratio is constant, the manoeuvre will follow one of the trajectories shown.
  b) When $\dot{\tau} > 1$, the aircraft is accelerating towards the goal and 2 solutions to $\omega_X \tau$ are possible, one with a positive frequency and the other with a negative frequency. The latter corresponds to unstable motion guides (negative stiffness).
  c) When $\dot{\tau} = 1$, $\omega_X \tau = -2\zeta_X$, indicating the transition between the acceleration and deceleration phases.
  d) The deceleration phase begins when $\dot{\tau} < 1$, $\dot{\tau}$ itself reaching a minimum value ($\dot{\tau} = 1 - \zeta_X^2$) when $\omega_X \tau = -\zeta_X$.

In Ref 6 it was shown how pilots can form a mental model of future motion using a, so-called, intrinsic tau-guide. Examples of potential motion guides are the constant deceleration, velocity and acceleration guides.

Constant velocity,

$$\tau_g = t - T, \qquad \dot{\tau}_g = 1 \qquad (14)$$

Constant deceleration,

$$\tau_g = \frac{1}{2}(t - T), \quad \dot{\tau}_g = 0.5 \qquad (15)$$

Constant acceleration,

$$\tau_g = \frac{1}{2}\left(t - \frac{T^2}{t}\right), \quad \dot{\tau}_g = \frac{1}{2}\left(1 + \left(\frac{T}{t}\right)^2\right) \qquad (16)$$

The constant velocity guide is a special case of the constant deceleration guide, with deceleration set to zero.

Tracking an intrinsic (mental model) tau-guide in the form,

$$\tau_x = k\tau_g \qquad (17)$$

where k is a constant, can help the pilot perform a deceleration (constant deceleration/velocity guide) or a complete accel-decel (constant acceleration guide). Note that the constant deceleration/velocity guide is asymptotic to the constant acceleration guide as τ approaches 0. Ref 6 shows data that illustrate very tight correlation between the aircraft motion and guides for both the stopping phase and the complete manoeuvre. The aircraft and guide start and finish together and approximate the constant relationship given by eqn (17) throughout the motion.

Motions connected through tau-coupling given by eqn (17) obey the power law relationship (Ref 7),

$$X = C\, X_g^{1/k} \qquad (18)$$

where C is a constant.

Normalising the distance and time by the manoeuvre length and duration respectively, the motion kinematics (for negative initial X) can be written as,

$$\overline{X} = -(1 - \bar{t}^2)^{\left(\frac{1}{k}\right)} \qquad (19)$$

$$\overline{X}' = \frac{2}{k}\bar{t}(1 - \bar{t}^2)^{\left(\frac{1}{k} - 1\right)} \qquad (20)$$

$$\overline{X}'' = -\frac{2}{k}\left[(\frac{2}{k} - 1)\bar{t}^2 - 1\right](1 - \bar{t}^2)^{\left(\frac{1}{k} - 2\right)} \qquad (21)$$

The motion gap closure rate ($\overline{X}'$) and acceleration ($\overline{X}''$) are shown in Figs 4 and 5. The closer k is to

unity the closer the trajectory mirrors the constant acceleration guide, with the closure rate increasing proportionately with time. For k close to unity, the maximum deceleration (maximum pitch up for the helicopter) occurs very late in the manoeuvre. A reducing k reflects a control strategy whereby the pilot elects to initiate the deceleration earlier in the manoeuvre.
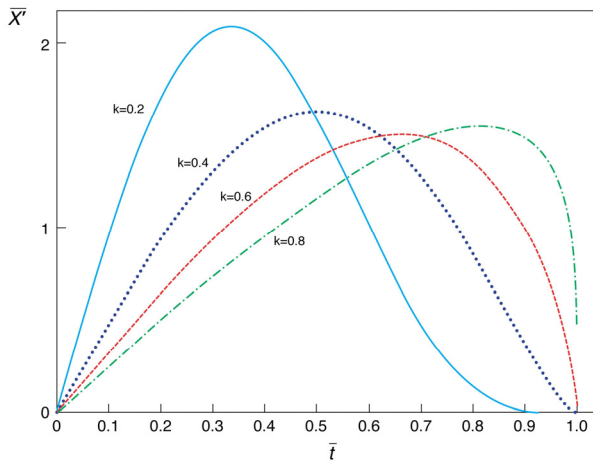

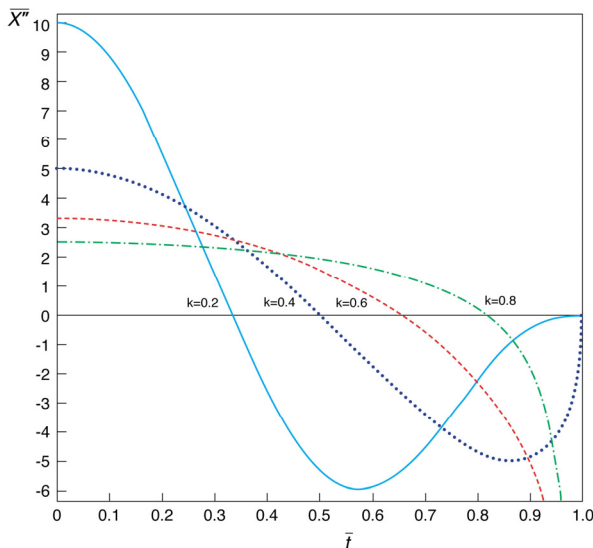**Figure 4 Kinematics of Motion following the Constant Acceleration Motion Guide – Closure rate**

Figure 5 Kinematics of Motion following the Constant Acceleration Motion Guide – Acceleration

It is useful to examine the nature of the variations in frequency and damping and corresponding pilot gains for control strategies that follow the different tau-guides. For the constant deceleration/velocity guide the pilot maintains $\dot\tau$ constant throughout the manoeuvre. This strategy can only be utilised when there is an initial velocity and not throughout the whole of the acceleration-deceleration manoeuvre. It can therefore be used by the pilot in the deceleration phase (see Refs 8-10 for examples of such motion guidance strategies in nature). Referring to eqn (13), and writing $\dot\tau - 1 = c$, a constant, then if we also assume that the damping is constant, ω_X is inversely proportional to the time to stop, τ. For the special case when $\zeta_X = \sqrt{0.5}$, and the stopping is conducted with a constant deceleration ($\dot\tau = 0.5$), we can write,

$$\omega_X = -\frac{0.707}{\tau} \qquad (22)$$

For this case, both the pilot range and velocity gains increase as the stopping point is approached, but the control 'law' given by eqn (1) must break down as the stopping point is reached, even though the gains can in principle reach high values. More generally, tau-theory hypothesises that the pilot is controlling the time gap, forcing a particular relationship between the damping and frequency given by eqn 13.

The constant acceleration tau-guide is more complex. In the very initial stages of the manoeuvre, when t<<T, eqn (16), combined with eqn (13) leads to the approximation,

$$\omega_X \approx -\frac{\sqrt{\dot\tau}}{\tau} \approx \frac{1}{T}\sqrt{\frac{2}{k}} \qquad (23)$$

This approximation indicates that the initial closed loop natural frequency is inversely proportional to the manoeuvre time. One might intuitively expect this, as the effective spring need not be strong if T is large (the commanded pitch angle would need to be unrealistically large). If the tau-coupling is weak (k small), then the pilot has elected to accelerate more rapidly initially, reaching the maximum velocity early in the manoeuvre, hence the inverse scaling with the coupling coefficient k. If we assume T = 20 seconds and k = 0.3 (values typical of an accel-decel), then ω_x = 0.13 rad/sec, a very similar value to that predicted by the constant $\dot\tau$ guidance model at the beginning of the deceleration phase (0.14=0.707/τ with time to stop = 5 seconds). The results suggest that the pilot

may adopt a strategy that keeps the positional gain constant (frequency remains constant) during the acceleration phase and then stiffens to a maximum as the hover is approached.

At the singular point when the acceleration ends and the deceleration begins, $\dot{\tau}=1$. From eqns (13) and (7), we can form the relationship between frequency and damping at this critical point,

$$\omega_X \tau = -2\zeta_X = -\frac{K_{\dot{X}}}{K_X}\omega_X \qquad (24)$$

At the point of reversal, the accelerative and braking components are equal and opposite. The time in the manoeuvre that the reversal occurs, t_r, can be derived as a function of the coupling coefficient k using eqn (16),

$$\dot{\tau}_g = \frac{k}{2}\left(1+\left(\frac{T}{t_r}\right)^2\right)=1 \qquad (25)$$

Eqn (25) can be re-arranged into the form,

$$t_r = \sqrt{\frac{k}{2-k}}\,T \qquad (26)$$

Thus when k = 0.2, t_r = 0.333T, when = 0.4, t_r = 0.5T and when = 0.6, t_r = 0.67T, etc.

The variation of ω and ζ for motion following the constant acceleration τ_g can be derived from the motion profiles in eqns (19) – (21). Re-arranging eqn (21) in terms of the closure rate and distance to go, the normalised acceleration can be written in the form;

$$\overline{X}'' = K_{\overline{X}}\,\overline{X} + K_{\overline{X}'}\,\overline{X}' \qquad (27)$$

where,

$$K_{\overline{X}} = \frac{2}{k\,(1-\bar{t}^2)^2} \qquad (28)$$

$$K_{\overline{X}'} = (\frac{2}{k}-1)\frac{\bar{t}}{(1-\bar{t}^2)} \qquad (29)$$

In these expressions time and distance are normalised by the manoeuvre time and distance respectively.

It follows that,

$$\overline{\omega}_{\overline{X}} = \sqrt{\frac{2}{k}}\,\frac{1}{(1-\bar{t}^2)} \qquad (30)$$

$$\overline{\zeta}_{\overline{X}} = \sqrt{\frac{k}{2}}\,(\frac{2}{k}-1)\bar{t} \qquad (31)$$

Figures 6 and 7 show the variations in the pilot gains, frequency and damping ratio as a function of normalised manoeuvre time.
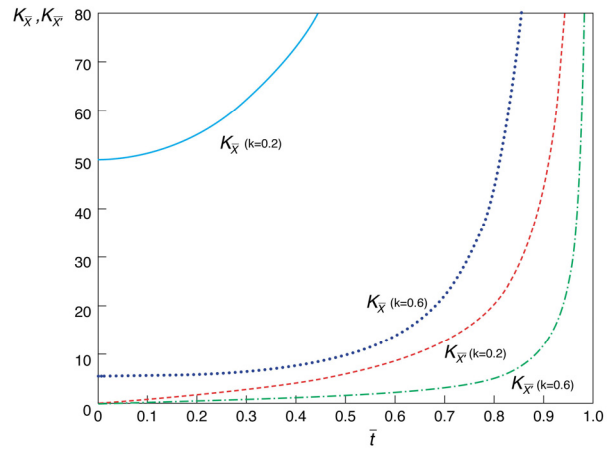

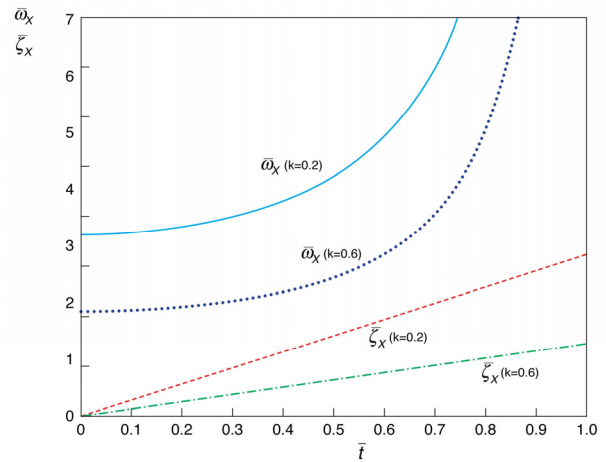**Figure 6 Variation of Pilot Gains with normalised manoeuvre time**

Figure 7 Variation of APM Frequency and Damping with normalised manoeuvre time

The frequency (range gain) stays fairly constant in the initial acceleration phase with the damping (velocity gain) increasing linearly. In the final stages of the deceleration, both gains increase sharply as the manoeuvre comes to a close.

It is useful to reflect on the analogy of the pilot as being in control of a spring and damper as feedback elements, each commanding a force guiding a mass from rest to rest. If, for example, the pilot chooses to hold a constant pitch attitude during the acceleration, the resulting constant acceleration could be achieved by applying a range gain inversely proportional to the distance to go. With this simple strategy, at the point of reversal the acceleration turns into a deceleration, the pitch attitude reverses and the proportional gain must change sign. The analogy is of the spring centre being at the point of reversal, and there is no requirement for the application of damping. However the APM then has no reference for the final stopping point. The combination of a rate and proportional feedback allows the resultant force to be either accelerative or decelerative. During the acceleration the spring draws the mass to the final resting position, the acceleration being attenuated by the damper. During the deceleration, the damper applies the braking force, with attenuation coming from the spring, which continues to draw the mass (helicopter) to rest (hover).

Several questions are raised by consideration of this analogy. For example, how do the different motion profiles relate to pilot workload when flying the accel-decel manoeuvre? How might this compare with the maximum performance profile? Relevant to the thrust of the current research, how does simulation fidelity influence the profiles. These questions are being addressed in the ongoing research.

Results from Piloted Simulations

The results presented in this section are for the FLIGHTLAB F-Bo105 helicopter (Fig 8) flown on the University of Liverpool's HELIFLIGHT facility (Fig 9, Refs 11, 12)).

Figure 8 DLR Research Bo105

Figure 9 The HELIFLIGHT Simulator

Two important handling qualities measures for flying the accel-decel manoeuvre are the moderate amplitude pitch attitude quickness (initial pitch down, reversal and final pitch up) and the small amplitude attitude bandwidth (final hover positioning). Figures 10 and 11 show comparisons of these parameters derived from the nonlinear F-Bo105 simulation and the DLR flight test data (Ref 13).
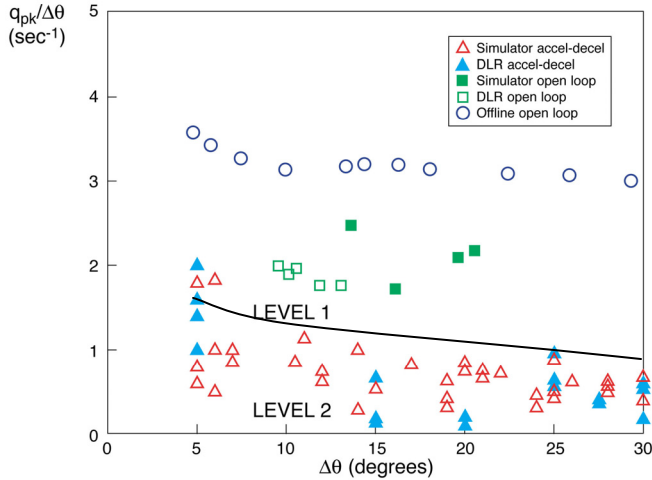
Figure 10 Bo105 Pitch Attitude Quickness

Fig 10 shows results for so-called open-loop tests (pilot applied pulse inputs in longitudinal cyclic) and also 'closed-loop' tests, derived from the accel-decel data. For the simulation, data are shown for pure pulse inputs (offline) and pilot applied inputs, which are more similar to the flight data. For attitude changes between 10 and 15 degrees the simulation derived (F-Bo105) quickness is about 25% higher than comparable data from flight. Similar levels of quickness are demanded by the pilot in both flight and simulation in the accel-decel manoeuvre. The attitude bandwidth and phase delay in Fig 11 also show a close agreement between flight and simulation.
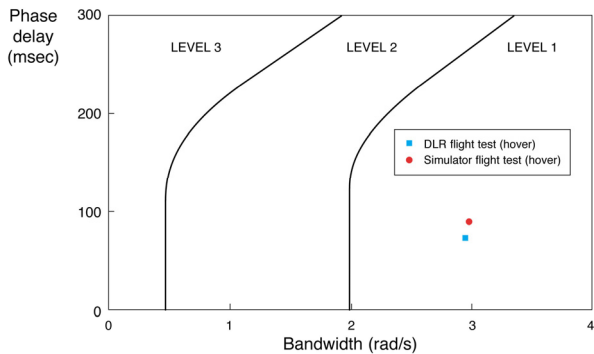
Figure 11 Bo105 Pitch Attitude Bandwidth

The results presented in this paper are taken from a trial where the pilot was required to fly a series of accel-decel manoeuvres with different visual and motion cueing arrangements and also various modelling changes. The visual scene content was defined by the levels of micro-texture (texture on surfaces) and macro-texture (physical objects).

Figures 12 and 13 show the views from the cockpit of the accel-decel course for the visual scenes designated as usable cue environment 1 and 3 by the test pilot (Refs 14, 15); the UCE 2 case included the 15 trees but no surface texture. The horizontal field of view is 135 degrees; the vertical field of view is 40 degrees on the 3 eye-level screens and 60 degrees for the lower chin windows. The stop position was located 1000 feet ahead of the start position and defined by the position of the final tree in the front window. The 50ft (~ 15m) high trees defined a corridor 150ft (~ 45m) wide. The task performance requirements are given in Table 1. The target maximum pitch attitude during both the acceleration and deceleration was 15 degrees, giving a horizontal accel/decel of about 0.25g. The results presented below are from configurations flown with response motion restricted to the pitch, heave and surge axes. The sway, roll and yaw degrees of freedom from the model outputs were locked. This subset of the total results gathered in the trial are the most coherent in terms of repeatability and statistical significance. Six runs for each configuration were flown by the test pilot and the results averaged.

Figure 12 Accel-Decel Course, UCE 1

Figure 13 Accel-Decel Course, UCE 3

	desired	adequate
Height	< 50ft(~ 15m)	< 70ft(~ 21m)
Heading	±10 deg	± 20 deg
Pitch angle	12 deg up, 15 deg down	7 deg up, 10 deg down

Table 1 Performance Standards in Accel-Decel

The averaged pitch attitude and horizontal (forward) velocity variations throughout the manoeuvre are shown in Figures 14 and 15.
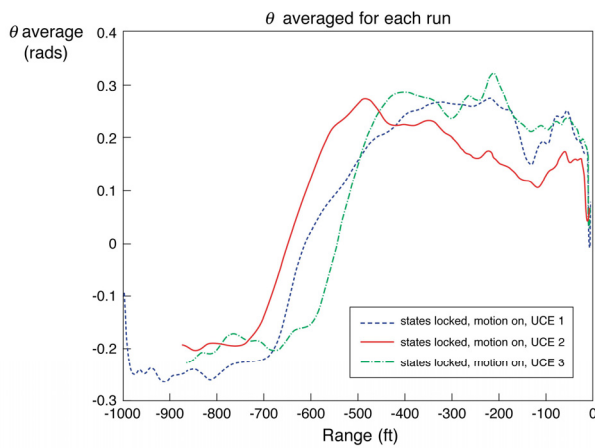
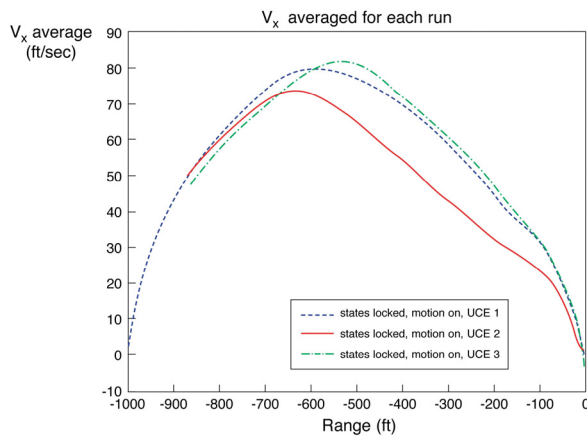

Figure 14 Attitude Profiles for Accel-Decels

Figure 15 Phase Plane Portraits for Accel-Decels

Figure 14 shows that the pilot has elected to hold a fairly constant (average) pitch attitude during both manoeuvre phases with (average) maximum

velocities between 70 and 80 ft/sec (~ 21 and 25m/sec).

Spatial Analysis

The method used to identify the pilot gains and associated APM frequency and damping involved fitting a (constant coefficient) 2nd order model (eqn 8) to the test data in 50ft (~ 15m) windows (20 across the manoeuvre). The final velocity and position for the motion in the nth window became the initial conditions for the n+1th window.

Figures 16-19 show the variations in estimated APM frequency, damping, range gain and velocity gain as a function of manoeuvre distance to go, for the 3 UCE cases. The overall shape of the functions is quite similar. The range gain and frequency remain fairly constant for the first 200 feet, increasing to a peak at the pitch reversal and decreasing again during the deceleration until the final stopping phase when the gain increases once more to about 0.3 deg/ft (~ 1 deg/m). The rate gain also increases to a maximum at the reversal and follows a similar pattern to the range gain at the manoeuvre end, leading to a levelling out of the relative damping as the manoeuvre comes to a close. The differences between the 3 UCEs is not particularly noticeable. There is some indication that the pilot has delayed the reversal until further into the manoeuvre for the UCE 3 case and also that the associated range gain (and damping) is lower at this point. The consequence of this more relaxed (careful) strategy is that the pilot then has to increase the braking action at the close of the manoeuvre with a relatively high range rate gain of about 1.3 deg/ft/sec (~ 4.3 deg/m/sec).
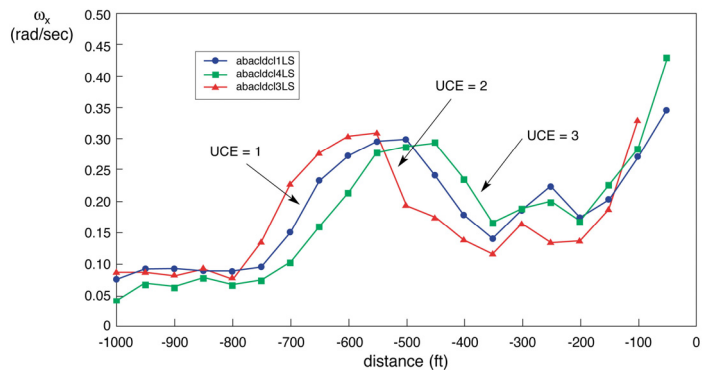

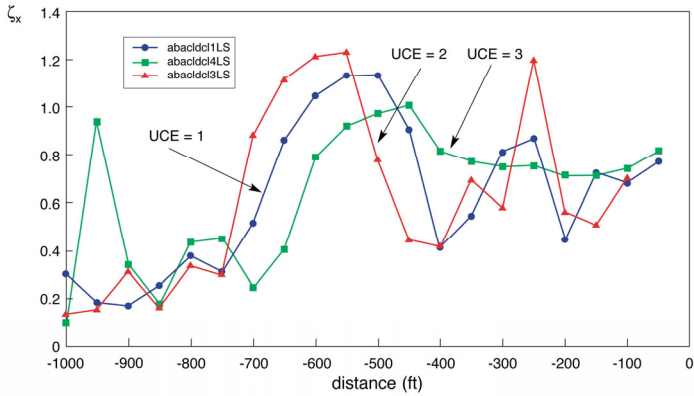**Figure 16 Variation of Frequency with Range for different UCEs**

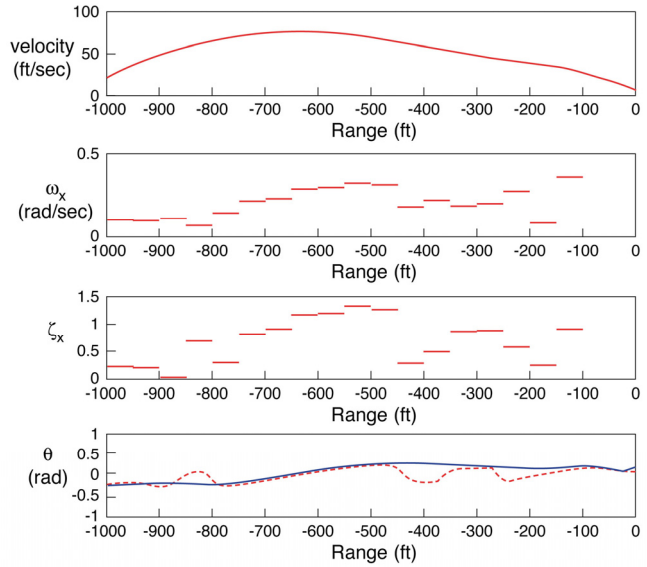**Figure 17 Variation of Damping Ratio with Range for different UCEs**

Figure 18 Variation of Range Gain with Range

Figure 19 Variation of Closure Rate Gain with Range

For all cases shown the re-constructed phase plane portraits (velocity vs distance to go) show a nearly perfect fit with the original data.

Figure 20 Re-Constructed Velocity and Pitch Attitude Variations (UCE1)

Figure 20 shows a sample comparison of the reconstructed velocity and pitch attitude for one of the UCE 1 cases. Also shown are the estimates of the varying frequency and damping for this run. In Fig 20, the reconstructed pitch attitude is actually the pitch attitude command θ_c derived from eqn 1.

The estimated θ_c follows the measured θ for much of the manoeuvre. Departures from this good tracking tend to coincide with marked deviations from the smooth variations in predicted damping; for example at the 850 ft point and again at the 400 ft point.
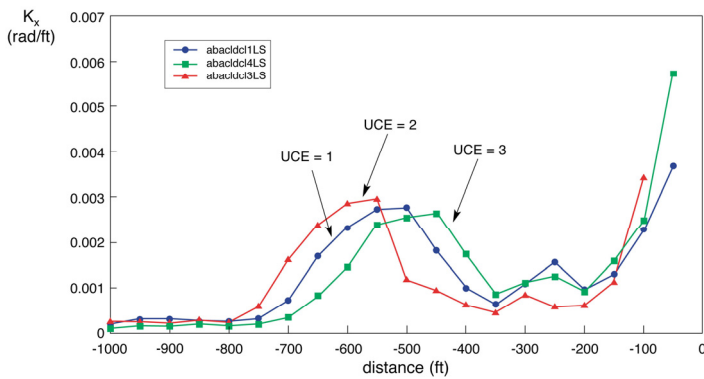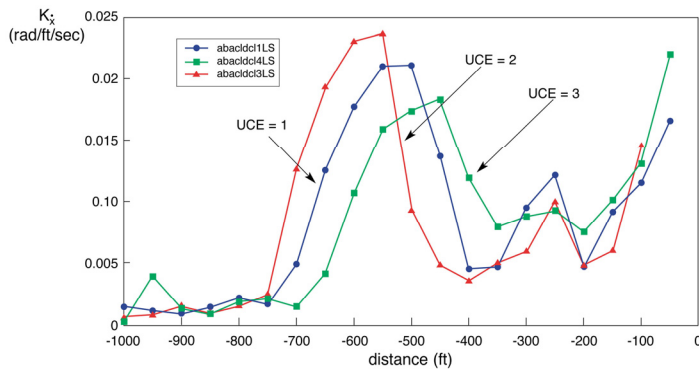
Temporal analysis

Fig 21 shows the fit of the averaged motion tau, τ_X, with the intrinsic guide tau, τ_g, the latter defined by the constant acceleration guide given in eqn. 16. The correlation coefficient, R^2, is greater than 0.98 for all three cases. The increased slope as UCE degrades is noted.
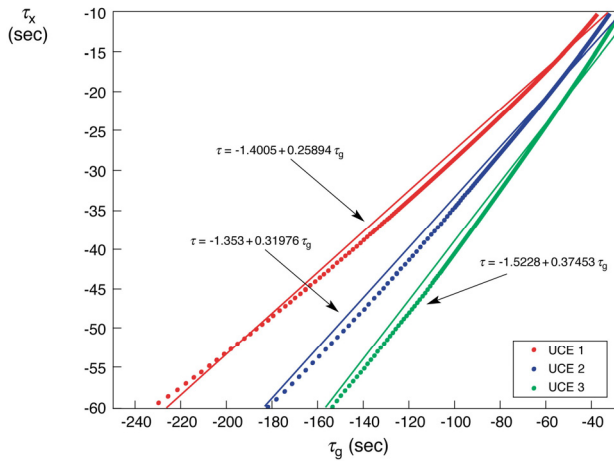
Figure 21 Example of Tau variations with Constant Acceleration Guide

Fig 22 shows the coupling coefficients (eqn 17) for the 18 individual accel-decels. While there are outlying data points for all three UCEs, there does appear to be a trend of increasing k with UCE, from 0.25 for UCE1, to 0.35 for UCE3 (also noted in Fig 21). Referring to Fig 4, this can be explained by the pilot delaying the pitch reversal further into the manoeuvre as the UCE degrades.
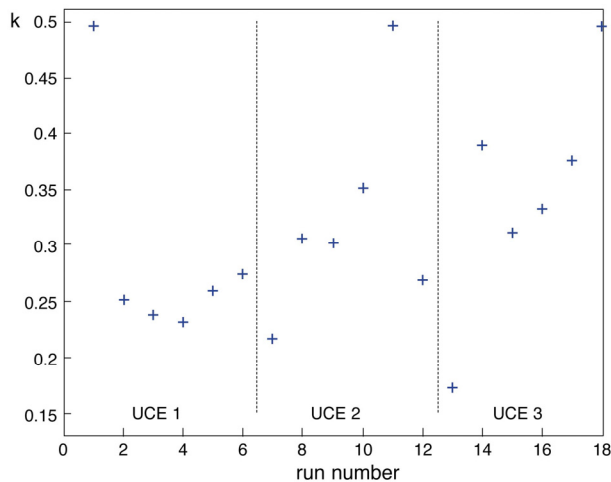

Figure 22 Tau-coupling coefficients for varying UCE

Using eqns 30 and 31, the variations in the APM frequency and damping can be derived for the temporal model. Figures 23 and 24 compare the predicted variations of ω_X and ζ_X, plotted against manoeuvre time, with those derived from the spatial model; one of the UCE1 cases is selected for this comparison, typical of most cases. The initial

variations compare well but the temporal model does not predict the rapid growth in both frequency and damping at the reversal and the consequent reduction. The temporal model predicts the increase only at the close of the manoeuvre, to much higher levels of frequency and damping than the spatial model.
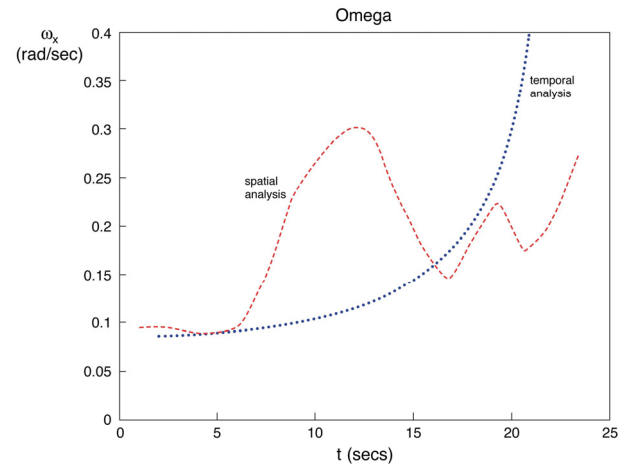

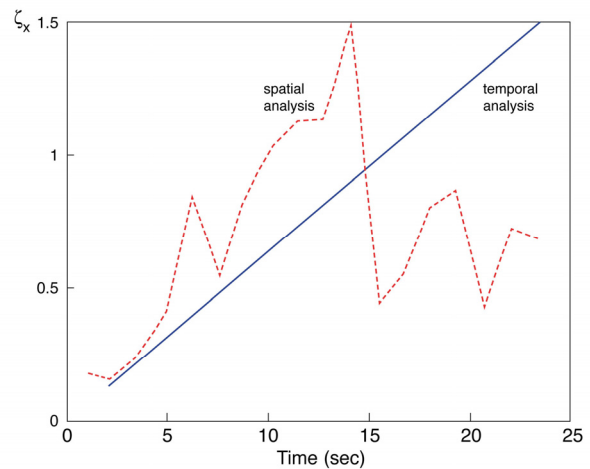**Figure 23 Comparison of Frequency estimations; spatial and temporal models (UCE1)**

Figure 24 Comparison of Damping Ratio Estimations; spatial and temporal models (UCE1)

Discussion

Both spatial and temporal models of the combined pilot-aircraft system capture the essential features of the dynamics in the acceleration-deceleration manoeuvre. The pilot applies the accelerator

during the acceleration, modulated by the brake and vice versa for the deceleration. There are differences between the two variants of the coupled behaviour models that are not fully reconciled at this stage in the research. The spatial model correctly predicts the evolving acceleration, assumed to be directly related to the pitch attitude. The pilot appears to prefer to maintain a relatively constant attitude during the acceleration and again during the deceleration. From Figs 16 and 17, it appears that a constant $\dot{\tau}$ guide is being followed in the deceleration (constant deceleration, $\dot{\tau}=0.5$); the frequency increasing sharply as the manoeuvre closes (inversely proportional to τ, see eqn 22). and damping staying relatively constant. Following the constant acceleration tau-guide, however, the predicted acceleration (see Fig 5) is actually much smoother, for the same performance than the spatial model predictions. Why the pilot has not chosen to follow the guide more tightly throughout the manoeuvre is not clear. This lingering question does raise a further question about what constitutes a minimum workload strategy and how the visual cues might affect this. In the cases presented in the paper, the manoeuvres were flown in different UCEs and the only noticeable effect was a delay in the point/time during the manoeuvre of the pitch reversal as the UCE degraded. This was also reflected in the tau-coupling coefficients increasing as UCE degraded. In all 3 cases, the APM gains predicted with the spatial model suggest that the pilot flies the manoeuvre in 2 distinct phases – the acceleration and the deceleration. The pitch reversal does, of course, present the pilot with a rather abrupt disruption to the flow of visual guidance information, the main 'screens' rotating 30 degrees in about 5 seconds and this may well explain the differences. In these few seconds the pilot has to focus on closing the θ gap, essentially a stabilisation task. The tau-guide following model implies a smoother pitch attitude change (see the k=0.2 line in Fig 5) throughout the manoeuvre. In the continuing research, different vehicle control models will be investigated, including the limiting case of the automobile-type (accelerator/brake) controls when no pitch attitude change is required, to investigate in more detail the impact of pitch motion on horizontal motion control.

The 2nd order model of motion control assumes that the stabilisation function takes place so quickly that there is a negligible impact on the guidance function. In practice it is known that the two functions can overlap as the level of manoeuvre aggressiveness or abruptness in increased (Ref 16). In the continuing research, a first step towards integrating both functions into the model will be to retain the 3rd order model given by eqn.6, hence introducing the parameter ω_θ, defining the bandwidth of the pilot attitude loop closure, into the model fit process.

At the time of writing, the DLR Bo105 flight test data is being prepared for equivalent analysis. The theoretical work presented in this paper forms the foundation for developing simulation fidelity criteria based on the difference between predicted parameters from simulation and flight. Results will be reported in the near future.

Concluding Remarks

This paper has reported progress in the developments of the Adaptive Pilot Model for capturing combined pilot-vehicle behaviour in manoeuvres. The initial focus has been on the low frequency guidance motion relevant to re-positioning manoeuvres. The acceleration-deceleration has been selected as the test case for these developments although the theory is applicable to the closing of any single degree of freedom 'gap'. Models based on both spatial control (proportional and rate feedback of distance to go) and temporal control (time to go) have been developed. The models have been exercised on accel-decel data captured in piloted simulations with 3 levels of visual cues, designated UCE 1, 2 and 3. Both spatial and temporal models of the combined pilot-aircraft system capture the essential features of the dynamics in the acceleration-deceleration manoeuvre. Differences between the two approaches have been highlighted however, the spatial model leading to closer fits with vehicle acceleration and pitch attitude. The temporal model on the other hand appears to be more sensitive to the UCE. The results suggest that the pilot may not actually be following the constant acceleration τ_g guide throughout the manoeuvre as theory would suggest; the pitch reversal effectively breaking the manoeuvre into two parts with the pilot following appropriate guides in each. The interpretation of these different results in terms of workload and performance is being studied in the continuing research. The theoretical developments provide the basis for conducting comparative assessments between flight and simulation data and thence to developing fidelity criteria based on the comparison of estimated model parameters.

Acknowledgements

References

1. Anon., JAR-STD 1H – Helicopter Flight Simulators, Joint Aviation Authorities, JAA, April 2001
2. Padfield, G.D., White, M., Simulation Fidelity Criteria using an Adaptive Pilot Model, 29th European Rotorcarft Forum, Friedrichshafen, Germany, Sept 2003 (*submitted to the Journal of Aerospace Science and Technology*)
3. McRuer, D.T., Krendel, E.S., Mathematical Models of Human Pilot Behaviour, AGARD AG 188, 1974
4. Heffley, R.K., A pilot-in-the-loop analysis of several kinds of helicopter acceleration-deceleration manoeuvres, NASA CP 2216, Helicopter Handling Qualities, 1982
5. Lee, D.N., The Optic Flow-field: the Foundation of Vision, Phil. Trans. R.Soc. London, B 290, 169-179, 1980
6. Padfield, G.D., Lee, D., Bradley, R., How Do Helicopter Pilots Know When to Stop, Turn or Pull Up? *(Developing guidelines for vision aids),* Journal of the American Helicopter Society, April 2003
7. Lee, D.N., Guiding Movement by Coupling Taus, Ecological Psychology, 10, 221-250, 1998
8. Lee, D.N., et al, Visual control of velocity of approach by pigeons when landing, Journal of Experimental Biology, 180, 85-104, 1993
9. Lee, D.N., et al, Aerial docking by hummingbirds, Naturwissenschaften, 78, 526-527, 1991
10. Lee, D.N., Reddish, P.E., Plummeting gannets: a paradigm of ecological optics, Nature, 293, 293-294, 1981
11. Padfield, G.D., White, M.D., Flight Simulation in Academia; HELIFLIGHT in its first year of operation, The Aeronautical Journal of the Royal Aeronautical Society, Vol 107, No 1075, Sept 2003
12. White, M.D., Padfield, G.D., Flight Simulation in Academia; Progress with HELIFLIGHT at The University of Liverpool, Flight Simulation 1929-2029: A Centennial Perspective, The Royal Aeronautical Society Flight Simulation Conference, London, May 2004
13. Ockier, C.J., Evaluation of ADS-33D handling qualities criteria using the Bo-105 helicopter, Forschungsbericht 98-07, DLR, Braunschweig, January 1998.
14. anon, Handling Qualities Requirements for Military Rotorcraft, Performance Specification, ADS-33-PRF, USAAMC, Aviation Engineering Directorate, March 2000
15. Padfield, G.D., Helicopter Flight Dynamics, Blackwell Science, Oxford, 1996
16. Padfield, G.D., et al., Where does the workload go when pilot attack manoeuvres?, An analysis from flying qualities theory and experiment, 20th European Rotorcraft Forum, Amsterdam, October 1994